Identifying precursors and aqueous organic aerosol formation pathways during the SOAS campaign

Neha Sareen[1], Annmarie G. Carlton[1, a], Jason D. Surratt[2], Avram Gold[2], Ben Lee[3], Felipe D. Lopez-Hilfiker[3, b], Claudia Mohr[3, c], Joel A. Thornton[3], Zhenfa Zhang[2], Yong B. Lim[1, d], Barbara J. Turpin[2]

1. Department of Environmental Sciences, Rutgers University, 14 College Farm Road, New Brunswick, New Jersey 08901, United States

2. Department of Environmental Sciences and Engineering, Gillings School of Public Health, University of North Carolina at Chapel Hill, Chapel Hill, North Carolina 27599, United States

3. Department of Atmospheric Sciences, University of Washington, Seattle, Washington 98195 United States

[a] Now at Department of Chemistry, University of California, Irvine, CA 92697, USA

[b] Now at Laboratory of Atmospheric Chemistry, Paul Scherrer Institute, 5232 Villigen PSI, Switzerland

[c] Now at Institute of Meteorology and Climate Research, Atmospheric Aerosol Research, Karlsruhe Institute of Technology, Karlsruhe, Germany

[d] Now at Center for Environment, Health and Welfare Research, Korea Institute of Science and Technology, Seoul 02792, Republic of Korea

Correspondence to: Neha Sareen (neha.sareen15@gmail.com), Barbara J. Turpin (bjturpin@email.unc.edu)

Abstract. Aqueous multiphase chemistry in the atmosphere can lead to rapid transformation of organic compounds, forming highly oxidized low-volatility organic aerosol and, in some cases, light-absorbing (brown) carbon. Because liquid water is globally abundant, this chemistry could substantially impact climate, air quality, and health. Gas-phase precursors released from biogenic and anthropogenic sources are oxidized and fragmented, forming water-soluble gases that can undergo reactions in the aqueous-phase (in clouds, fogs, and wet aerosols) leading to the formation of secondary organic aerosol (SOA_{AQ}). Recent studies have highlighted the role of certain precursors

like glyoxal, methylglyoxal, glycolaldehyde, acetic acid, acetone, and epoxides in the formation of SOA_{AQ}. The goal of this work is to identify additional precursors and products that may be atmospherically important. In this study, ambient mixtures of water-soluble gases were scrubbed from the atmosphere into water at Brent, Alabama during the 2013 Southern Oxidant and Aerosol Study (SOAS). Hydroxyl (OH•) radical oxidation experiments were conducted with the aqueous mixtures collected from SOAS to better understand the formation of SOA through gas-phase followed by aqueous-phase chemistry. Total aqueous-phase organic carbon concentrations for these mixtures ranged from 92-179 μM-C, relevant for cloud and fog waters. Aqueous OH-reactive compounds were primarily observed as odd ions in the positive ion mode by electrospray ionization mass spectrometry (ESI-MS). Ultra high-resolution Fourier-transform ion cyclotron resonance mass spectrometry (FT-ICR-MS) spectra and tandem MS (MS/MS) fragmentation of these ions were consistent with the presence of carbonyls and tetrols. Products were observed in the negative ion mode and included pyruvate and oxalate, which were confirmed by ion chromatography. Pyruvate and oxalate have been found in the particle phase in many locations (as salts and complexes). Thus, formation of pyruvate/oxalate suggests the potential for aqueous processing of these ambient mixtures to form SOA_{AQ}.

1 Introduction

Aqueous multiphase chemistry has the potential to alter the climate-relevant properties and behavior of atmospheric aerosols. It is well-established that a major pathway for secondary organic aerosol (SOA) formation is via the partitioning of semi-volatile products of gas-phase photochemical reactions into preexisting organic particulate matter (Seinfeld and Pankow, 2003). Semi-volatile partitioning theory is widely used to model SOA (Odum et al., 1996; Seinfeld and Pankow, 2003; Donahue et al., 2006). However differences between organic aerosol mass/properties predicted via this formation mechanism and those measured in the atmosphere suggest that other

processes (e.g., aqueous chemistry) may also contribute (Foley et al., 2010; Hallquist et al., 2009).

Recent studies have highlighted the importance of water-soluble organic gases (WSOGs), liquid water, and condensed-phase reactions to SOA formation and properties (Ervens et al., 2011; Monge et al., 2012; Carlton and Turpin, 2013). Biogenic and anthropogenic gas-phase precursors are oxidized to form WSOGs such as glyoxal, methylglyoxal, glycolaldehyde, and acetone (Spaulding et al., 2003). These WSOGs are too volatile to form SOA through absorptive partitioning, but they can undergo aqueous reactions in clouds, fogs, and wet aerosols to form low-volatility products and "aqueous" SOA (SOA_{AQ}) (Blando and Turpin, 2000; Ervens et al., 2004; Kroll et al., 2005; Liggio et al., 2005; Lim et al., 2005; Heald et al., 2006; Loeffler et al., 2006; Sorooshian et al., 2006; Volkamer et al., 2006; Volkamer et al., 2007; Ervens et al., 2008; De Haan et al., 2009a; El Haddad et al., 2009; Ervens et al., 2011; Rossignol et al., 2014). Inclusion of aqueous chemistry of clouds, fogs, and wet aerosols in models and experiments helps to explain discrepancies in atmospheric observations of SOA that are not explained by semi-volatile partitioning theory, particularly high atmospheric O/C ratios, enrichment of organic aerosol aloft, and formation of oxalate, sulfur- and nitrogen-containing organics and high molecular weight compounds (Kawamura and Ikushima, 1993; Kawamura et al., 1996; Crahan et al., 2004; Kalberer et al., 2004; Herrmann et al., 2005; Altieri et al., 2006; Carlton et al., 2006; Heald et al., 2006; Volkamer et al., 2007; Nozière and Cordova, 2008; De Haan et al., 2009b; El Haddad et al., 2009; Galloway et al., 2009; Shapiro et al., 2009; Volkamer et al., 2009; Lim et al., 2010; Lin et al., 2010; Nozière et al., 2010; Perri et al., 2010; Sareen et al., 2010; Schwier et al., 2010; Sorooshian et al.,

80   2010; Sun et al., 2010; Ervens et al., 2011; Lee et al., 2011; Tan et al., 2012; Ervens et al., 2013; He et al., 2013; Gaston et al., 2014; Ortiz-Montalvo et al., 2014). Although uncertainties are large, modeling studies show that SOA_{AQ} is comparable in magnitude to "traditional" SOA (Carlton et al., 2008; Fu et al., 2008; Fu et al., 2009; Gong et al., 2011; Myriokefalitakis et al., 2011; Liu et al., 2012; Lin et al., 2014). However, SOA_{AQ}

85   precursors and their chemical evolution remain poorly understood.

Much of what we know about aqueous chemistry leading to SOA_{AQ} formation is derived from laboratory studies with single precursors hypothesized to be important; however, the most important precursors for SOA_{AQ} formation in the ambient environment may remain unidentified. A small number of studies conducted with

90   ambient mixtures have provided insights into the pathways of SOA_{AQ} formation. For example, photochemical oxidation of aerosol filter samples and cloud water from Whistler, British Columbia suggest that water-soluble organic compounds of intermediate volatility (e.g. *cis*-pinonic acid) can be important precursors for SOA_{AQ} (Lee et al., 2012). Pyruvic acid oxidation experiments in Mt. Tai, China cloud water suggested a slowing of

95   pyruvic acid oxidation presumably due to competition for OH radicals with the complex dissolved cloud water organics (Boris et al., 2014). However, further ambient measurements are needed to identify precursors important for ambient SOA_{AQ} formation in atmospheric waters.

This work reports, for the first time, results of aqueous OH radical oxidation

100   experiments conducted in ambient mixtures of water-soluble gases. Ambient mixtures were collected in the southeast US during the Southern Oxidant and Aerosol Study (SOAS) in the summer of 2013; experiments were used to identify water-soluble gases

that may serve as precursors of atmospheric aqueous SOA. This region has experienced

an overall cooling trend in surface temperature over the second half of the twentieth

century, compared to the warming trend observed elsewhere in the US (Robinson et al.,

2002; Goldstein et al., 2009; Portmann et al., 2009). Biogenic sources dominate

emissions in this region with varying degrees of impact from anthropogenic sources.

Measurements by Nguyen et al. (2014) and model results by (Carlton and Turpin, 2013)

indicate the significance of anthropogenic aerosol liquid water (ALW) in this region and

support a role for ALW in SOA_{AQ} formation. In the southeast US, photochemistry and

abundant liquid water coexist, making it an ideal location to study SOA_{AQ} formation

through gas-phase followed by aqueous-phase chemistry. The objective of this work is to

identify WSOGs important to SOA_{AQ} formation. Since OH oxidation experiments were

conducted in dilute solution, we will also identify products expected through cloud/fog

processing of ambient WSOG mixtures. Products may differ in aerosols, where solute

concentrations are higher, and radical-radical chemistry and acid-catalyzed reactions (e.g.

epoxide ring-opening reactions yielding tetrols and organosulfates from isoprene

epoxydiol, IEPOX) are important. We expect that aqueous chemistry in clouds, fogs, and

wet aerosols is a sink for reactants identified herein, and that this work will motivate

laboratory studies and chemical modeling of newly identified aerosol/cloud precursors.

2 Methods

Samples of ambient water-soluble mixtures collected in mist chambers during the

SOAS field study were used to conduct controlled aqueous OH radical oxidation

experiments. Mass spectral techniques were used to tentatively identify compounds with

decreasing abundance in aqueous OH oxidation experiments, but not control experiments with the aim of identifying new aqueous chemistry precursors for further study. Ion chromatography was used to identify selected products.

2.1 Mist chamber field sampling at SOAS (in Brent, AL)

Water-soluble gases were scrubbed from filtered ambient air at the Centerville ground site in Brent, AL during SOAS. Samples were collected from June 1 – July 14, 2013 from 1 m above the sampling station roof through a 1.3 cm OD Teflon inlet (approximately 1.7 m in length). Four mist chambers (Anderson et al., 2008a; Anderson et al., 2008b; Dibb et al., 1994; Hennigan et al., 2009) were operated in an air-conditioned trailer (indoor temperature, 25°C) at 25 L min^{-1} in parallel for 4 hours, typically 2-3 times each day between 7 AM and 7 PM CDT. Particles were removed by passing the ambient air through a pre-baked quartz fiber filter (QFF) (Pall, 47mm) prior to introduction into the mist chamber.

The mist chambers were operated with 25 mL of 17.5 ± 0.5 MΩ ultra-pure water; additional water was added during the run to replace water lost by evaporation. Samples from all four mist chambers were composited daily and frozen in 35 – 40 mL (experiment-sized) aliquots. Total organic carbon (TOC) concentrations ranged from 45 – 180 μM-C (Supplementary Table S1). Prior to and at the end of a sampling day, each mist chamber was cleaned using a 5-minute DI water wash step.

Based on daily forecast predictions, certain days were selected for intensive sampling (Supplementary Table S1). Intensive sampling during SOAS was conducted on days when high levels of isoprene, sulfate, and NO$_x$ were predicted by the National

Center for Atmospheric Research (NCAR) using the Flexible Particle dispersion model

150   (FLEXPART) (Stohl et al., 2005) and the Model for Ozone and Related Chemical

Tracers (MOZART) (Emmons et al., 2010). In general, mist chamber samples on

intensive sampling days had higher organic content (TOC = 92-179 µM-C), and hence

we focused our experiments on those days and included two additional days from the

non-intensive period that had high TOC values (Table 1).

155

2.2 Aqueous OH radical oxidation in a cuvette chamber

Ambient SOAS field samples were exposed to OH radicals in a custom built

photochemical temperature-controlled (25°C) quartz cuvette reaction chamber. Ten

screw-capped quartz cuvettes (Spectrocell Inc., Oreland, PA) containing 3 mL of sample

160   were placed equidistant around a 254 nm mercury lamp (Heraeus Noblelight, Inc. Duluth,

GA) housed in a quartz sheath (Ace Glass Inc., Vineland, NJ). A solar spectrum lamp

was not used because the objective was to produce OH radicals by H_2O_2 photolysis,

rather than to mimic tropospheric photolysis. The chamber was protected from ambient

light by covering in aluminum foil. OH radicals (1.25×10^{-2} µM [OH] s^{-1}) were generated

165   *in situ* by photolysis of 125 µM H_2O_2, added to each cuvette prior to inserting the lamp.

While we can calculate the OH production rate from hydrogen peroxide photolysis

(1.25×10^{-2} µM [OH] s^{-1}), the concentration of OH in the reaction vessel depends also on

the reactivity of the organics. If the WSOG mix behaves similarly to glyoxal, OH

concentrations would be on the order of 10^{-12} M (similar to Tan et al., 2009). Cuvettes

170   were removed at t = 10, 20, 30, 40, 60, 80, 100, 120, 150 min and any remaining H_2O_2

was destroyed by addition of 36 µL of 1% catalase (Sigma; 40,200 units/mg). A duplicate

cuvette was removed at t = 40 min to calculate method precision. The following control experiments were performed: 1) sample + H_2O_2, 2) sample + UV, 3) H_2O_2 + UV, and 4) field water blank + OH. Replicate experiments were performed on selected samples. Ambient conditions for sample collection are given in Table 1 for samples used in experiments.

2.3 Analytical methods

Samples and field water blanks from all collection days were characterized by total organic carbon analysis (TOC; Shimadzu 5000A) and electrospray ionization mass spectrometry (ESI-MS; HP – Agilent 1100). Ion Chromatography (IC; Dionex ICS 3000) was used to analyze organic anions and track the formation of products and intermediates. Samples at each reaction time were analyzed by ESI-MS in positive and negative ion modes to identify precursors and products. Selected samples were also analyzed by ultra-high resolution electrospray ionization Fourier-transform ion cyclotron resonance mass spectrometry (ESI-FT-ICR-MS) and tandem MS (MS-MS) on a Thermo-Finnigan LTQ-XL at Woods Hole Oceanographic Institute, MA to determine elemental composition and extract structural information on precursors. Analytical details and quality control measures have been described previously (Perri et al., 2009). Briefly, the ESI quadrupole mass spectrometer was operated in positive and negative ion modes over a mass range of 50-1000 amu. In the negative ion mode, the mobile phase consisted of 1:1 methanol/0.05% formic acid in water; and in the positive ion mode, 0.05% formic acid in water. The fragmentor and capillary voltages for the ESI-MS were set at 40 V and 3000 V (nitrogen drying gas; 10 L min^{-1}; 350 °C), respectively. Nitrobenzoic acid in the

195   negative ion mode and caffeine in the positive ion mode were used as mass calibrants. Standard mixtures were analyzed with each experimental sequence: acetic acid, pyruvic acid, nitric acid, succinic acid, tartaric acid, ammonium sulfate, and oxalic acid in the negative ion mode and glyoxal, methylglyoxal, and glycolaldehyde in the positive ion mode.

200   ESI ionization efficiency varies with sample mix and over time. However, the mass spectra of the mist chamber samples were similar across experimental days and the variability in the glyoxal, methylglyoxal, and glycolaldehyde standard ESI signals were 4-7% across analysis days, suggesting that ion abundance trends (Figure S1-S2) will reflect concentration trends. Six injections were averaged for each sample and data

205 retained for each ion abundance greater than zero within 95% confidence intervals. Ions were considered to be above detection limits if peaks were greater than the average plus three standard deviations of the water blank.

      Organic acids were measured by IC (IonPac AS11-HC column; 30 °C, AG11-HC guard column) with conductivity detection (35 °C), using a Milli-Q water eluent and

210 KOH gradient method. For oxalate, the method precision is 22%, calculated as a pooled coefficient of variation (CV) from pairs of cuvettes removed at t=40 min. The analytical precision for oxalate is 19% (pooled CV) based on replicate analysis of 30% of samples. Analytical accuracy for oxalate is 7%. The limit of detection (LOD) for oxalate by this protocol has been previously determined to be 0.1 µM (Perri et al., 2009).

215   Samples from June 15 and June 30, 2013 were analyzed using ultra-high resolution FT-ICR-MS in the positive ion mode using 1:1 methanol/water as the mobile phase at 4 µL min^{-1}, capillary temperature of 260 °C and spray voltage 3.8-4.2 kV.

Weekly analysis of standards (caffeine, peptide-MRFA, ultramark, SDS, and sodium taurocholate) verified the mass accuracy < 2 ppm. Previously pyruvic acid and

220   peroxyhemiacetal standards analyzed with the same protocol were within 2 - 10 ppm. Five precursor masses were isolated (isolation width: $m/z = 2$) and fragmented by collision-induced dissociation (CID) (normalized collision energy: 26-33%) with helium in the ion trap (IT) and infrared multi photon dissociation (IRMPD) with a CO_2 laser. Elemental composition (within ±1 ppm) and double bond equivalents of ions were

225   calculated by Midas Molecular Formula Calculator (v1.1). No restrictions were placed on the number of carbon, hydrogen, oxygen, nitrogen, sodium, and sulfur atoms included in the molecular formula calculations.

Compounds are detected in the ESI-MS by forming cluster ions with hydrogen, sodium, or ammonium in the positive ion mode; compounds are sometimes hydrated with

230   water or methanol. In the negative ion mode, ions are deprotonated.

3 Results & Discussion

OH oxidation experiments at concentrations relevant to cloud/fog water were conducted on samples collected June 11, 12, 15, 16, 20, 21, 29, and 30 of 2013, days on

235   which total organic carbon (TOC) was highest, ranging from 92-179 µM-C in samples.

3.1 Precursors in SOAS samples

The concentration dynamics in experiments conducted with the 8 daily composites were similar. Positive ions at m/z 125, 129, 143, 173, and 187 exhibited

240   reactant-like trends (Figure 1; June 30 sample + OH), showing decreasing signal intensity

with increasing exposure to OH. These ions disappeared after 40 minutes of oxidation. Together, these ions account for roughly 30% of the total ion current in the positive mode in the experiment samples. In control experiments, the abundance of these ions did not change over time, as illustrated in Figure 1 (sample + UV and sample + H_2O_2) for the positive ion at *m/z* 187 in samples collected on June 15 and 30. Hence, reaction with UV or H_2O_2 alone does not explain the decreasing signals in the presence of OH radical. In control experiments where we generated OH radicals in field water blanks, these ions were not observed, confirming that they are not contaminants. Experiments conducted on all sample days showed the same reactants decreasing with exposure to OH, indicating that the water-soluble organics captured from the ambient daytime air in the mist chambers varied little across the study.

Elemental formulae assigned to precursor ions by Midas with corresponding MS-MS fragmentation data for the ions from June 15 and 30 samples are shown in Table 2. Both sampling days showed similar fragmentation spectra, consistent with the presence of the same parent compounds on both days, despite potential differences in the air mass on these days. MS-MS spectra were not obtained under the acquisition conditions of this work for positive ions at *m/z* 143, 129 and 125. Proposed structures for the positive ions at *m/z* 187 and 173 based on MS-MS data are shown in Figures 2 and 3 The O:C ratio for the reactant masses range from 0.1 - 0.8. In the following sections, we discuss individual reactants observed by ESI-MS. The discussion below is focused on the molecular formulas, rather than the detected ions, i.e. Na^+ or H^+.

m/z 187: This is the ion with the highest *m/z* observed by ESI-MS in the positive ion mode that follows a precursor-like trend (Figures 1 and 2). The composition

$C_7H_{16}O_4Na$ is assigned by the Midas molecular formula calculator based on the exact
mass 187.0942 from FT-ICR MS, corresponding to the composition $C_7H_{16}O_4$ for the
neutral compound. The MS-MS shows loss of methanol, to give a product ion at m/z
155.0680 corresponding to the neutral molecular formula, $C_6H_{12}O_3.$, consistent with
expectations for a sodium ion complex of a dihydroxy hemiacetal in methanol solution,
shown in Figure 2. In the absence of methanol, this compound would appear hydrated
with water as the $C_6H_{14}O_4$ tetrol, as shown in the blue box in Figure 2. The corresponding
gas-phase compound is shown in the tan box in Figure 2.

E-2-hexenal and Z-3-hexenal are unsaturated aldehydes that have frequently been
detected during field studies and are emitted to the atmosphere from vegetation due to
leaf wounding (O'Connor et al., 2006). The gas-phase oxidation of these two green leaf
volatiles, as shown in Figure 4a and 4b, could explain the presence of $C_6H_{12}O_3$ in the gas-
phase and $C_6H_{14}O_4$ in the aqueous-phase (Figure 2).

m/z 173: On most sampling days this reactant mass has the highest abundance in
the positive mode ESI mass spectra (Supplementary Figure S1). Similar to other reactant
peaks, it reacts away within the first 40 minutes of exposure to OH in the cuvette
chamber (Figure 1). The Midas-suggested molecular formula for this parent ion (m/z
173.0782) and its two fragment ions at m/z 141.0523 and 129.0524 are $C_6H_{14}O_4$,
$C_5H_{10}O_3$, and $C_4H_{10}O_3$, respectively (a reactive parent ion with the formula $C_4H_{10}O_3$ was
also observed, and is discussed below).

A likely structure for positive mode m/z 173 is shown in Figure 3. In this case the
compound is proposed to be a $C_5H_{10}O_3$ aldehyde in the gas-phase (tan box in Figure 3)
and a $C_5H_{12}O_4$ tetrol in water (blue box in Figure 3). In the FT-ICR-MS it is seen

hydrated with methanol. The parent ion at *m/z* 173 loses methanol to form $C_5H_{10}O_3$ (*m/z* 141.0523), and it also loses C_2H_4O to form $C_4H_{10}O_3$ (*m/z* 129.0524). The aqueous oxidation precursor observed as m/z+ 173 and tentatively identified as the $C_5H_{10}O_3$

290   aldehyde shown in tan in Figure 3, could be derived from another green leaf volatile. Specifically, $C_5H_{10}O_3$ is consistent with the gas-phase oxidation product of (*E*)-2-methyl-2-butenal, another green leaf volatile (Figure 4c) (Jiménez et al., 2009; Lanza et al., 2008).

Positive ions at m/z 143, 129, and 125: No fragments were observed for these

295   reactants under conditions of MS-MS acquisition in this work. The Midas-predicted molecular formulae for the ions at *m/z* 143.0676, 129.0520, and 125.096 are $C_5H_{12}O_3$, $C_4H_{10}O_3$, and $C_8H_{12}O$, respectively. Interestingly, the reactant detected at *m/z* 129 has the same mass as a fragment of the parent ion at *m/z* 173 discussed earlier (and the structure of the $C_4H_{10}O_3$ fragment shown in Figure 3 is a possible structure for *m/z* 129).

300   *Methodological Limitations:* In this work, we aim to collect the ambient mix of water-soluble gases into water at concentrations comparable to those found in clouds and fogs with the purpose of simulating cloud/fog-relevant OH oxidation chemistry and identifying previously unrecognized precursors of aqueous chemistry. Below we discuss limitations with respect to our ability to collect and store these aqueous mixtures and with

305   respect to our ability to identify the OH-reactive compounds collected.

Mist chamber collection times (4 hr) were selected with the aim of collecting ambient mixtures of water-soluble gases near Henry's law equilibrium. Two pieces of evidence suggest that gas-aqueous partitioning of the WSOGs is close to Henry's Law equilibrium in our samples. In previous testing conducted in a different East Coast

310   location that is a recipient of long-range transport (i.e., central New Jersey), we found

that WSOG concentrations in the mist chamber leveled off after 1-3 hours of ambient

sampling, suggesting that the collected WSOG mixture approaches Henry's Law

equilibrium over these collection times. This is consistent with the one measurement we

have of breakthrough at SOAS, where we ran two mist chambers in series and found

315   TOC concentrations within +/- 11% of each other. These measurements suggest that a

representative mixture of the water-soluble gases entering the mist chambers were

collected.

However, WSOGs can be lost during sampling and storage through: 1) losses in

tubing and by adsorption to the QFF during collection, 2) reactions in the mist chamber

320   during collection with water-soluble ambient oxidants capable of penetrating the inlet

(e.g., ozone), and 3) losses during storage post collection. The QFF removes particles

upstream of the mist chambers. In the early stages of sampling, on the clean filter,

adsorption of gases on the filter will reduce the concentrations of gases sampled by the

mist chamber until these gases reach gas-phase − adsorbed-phase equilibrium. Using

325   glyoxal as a WSOG-surrogate and the work of (Mader and Pankow, 2001) we predict

that the measured WSOG in the mist chamber will be depleted for less than 2% of our

sampling time (after <0.1 m^3) due to loss to the filter. Thus, we expect water-soluble

gases to penetrate through the QFF very efficiently for collection in the mist chamber

water. Losses to Teflon inlets and chamber walls (Krechmer et al., 2016) can be

330   significant and variable and may reduce the number of species we are able to collect and

identify in this work. While OH radicals are unlikely to penetrate the inlet, ozone might.

Thus some ozone could be scrubbed by the mist chambers and could result in oxidation of some unsaturated WSOGs during collection.

Though many organics are stable when stored frozen in water, IEPOX does not survive extended storage in water (confirmed with our organic synthesis collaborator). We expect this to be the case for isoprene hydroxyhydroperoxide (ISOPOOH) also. ISOPOOH is an OH oxidation product of isoprene, which is further oxidized by OH under low-NO conditions to form isomeric IEPOX (Paulot et al., 2009). IEPOX and ISOPOOH were present in the gas-phase during the SOAS campaign (Nguyen et al., 2015). They have relatively high Henry's Law constants (i.e., ($H_{L,IEPOX}$=2.7 x 10^6 M atm^{-1}). IEPOX was readily detected in ambient samples spiked with 3000 μM, 300 μM, and 30 μM of IEPOX, indicating that it can be ionized in our sample matrix. (Authentic *trans*-β-IEPOX, which is the predominant isomer of IEPOX, was synthesized for this purpose (Zhang et al., 2012).) However, it was not found in our ambient samples since it is not stable when stored in water.

Together, the ions discussed herein account for 30% of the total ion abundance. The remaining 70% did not exhibit a clearly decreasing trend during OH oxidation experiments. It should be recognized that some water-soluble OH-reactive compounds might not have decreased during experiments because they were intermediates of multiple precursors. Together, these methodological limitations suggest that additional OH-reactive water-soluble gases were likely present that we were unable to identify.

3.2 Product formation during aqueous oxidation experiments

355   Figure 5 shows significant formation of oxalate and pyruvate in OH radical experiments conducted with all samples but not during the control experiments (Sample + UV; Sample + H_2O_2). Pyruvate peaks around 60-80 min, which is earlier than the oxalate peak at 100-120 min (Figure 5). Acetate + glycolate (which co-elute in the IC) also forms in at least some samples and reacts away in the presence of OH (Supplementary Figure

360   S3). Sulfate and nitrate concentrations remained constant throughout the experiment as measured by the IC. While there may be many sources of oxalate, aqueous OH radical oxidation of pyruvate in the aqueous-phase is known to form oxalate at dilute (cloud-relevant) concentrations (Carlton et al., 2006). Aqueous acetate oxidation is also a source of oxalate (Tan et al., 2012). The concentration dynamics are consistent with a role for

365   these compounds in the formation of oxalate in the ambient mixtures although the mechanisms by which pyruvate and acetate formed are not well constrained in these experiments. These observations suggest that oxalate, pyruvate, and acetate/glycolate can form in ambient mixtures of water-soluble gases in the southeast US in the presence of clouds/fogs and oxidants. Pyruvate and oxalate have been observed primarily in the

370   particle phase in the atmosphere (Saxena and Hildemann, 1996; Limbeck et al., 2001; Yao et al., 2002; Kawamura et al., 2003; Martinelango et al., 2007). Moreover, modeling studies of oxalate, the most abundant dicarboxylic acid in the atmosphere, suggest that aqueous chemistry is a large contributor of oxalate formation globally, making it a good tracer for SOA_{AQ} formed in clouds and fogs (Myriokefalitakis et al., 2011). Above versus

375   below cloud measurements also support this (Sorooshian et al., 2010). Thus, the experiments suggest that aqueous oxidation of ambient (southeastern US) water-soluble mixtures at cloud/fog relevant concentrations has the potential to form material that

remains in the particle-phase species after droplet evaporation, i.e. SOA_{AQ}. However, the atmospheric prevalence of *particle-phase* oxalate can only be explained by the formation

380   of salts and complexes, since oxalic acid is volatile and the volatility of oxalate salts is orders of magnitude lower than that of oxalic acid (Ortiz-Montalvo et al., 2014; Paciga et al., 2014). The aerosol at the SOAS ground site was acidic (campaign average pH~0.94) (Guo et al., 2015) and as a consequence oxalic acid may remain largely in the gas-phase in this environment, but may eventually react on more basic surfaces, e.g., coarse

385   particles. Note that we expect the products of aqueous chemistry in wet aerosols to be different from those in clouds and fogs because of the extremely high (molar) solute concentrations in wet aerosols (Surratt et al., 2007; Noziere et al., 2008; Galloway et al., 2009; Lim et al., 2010; Sareen et al., 2010; Nguyen et al., 2012).

390   **3.3 Atmospheric implications**

We have tentatively characterized several water-soluble OH-reactive species collected at an isoprene-rich photochemically-active location in the southeastern U.S. In several cases compounds with the same elemental composition were measured in the gas-phase by HRToF-CIMS. The tentative structures for the proposed reactants are consistent

395   with formation from green leaf volatiles and isoprene oxidation. Aqueous OH oxidation under dilute conditions (TOC approx. 100 μM) relevant to fogs and clouds produced oxalate and pyruvate suggesting that cloud/fog processing of these compounds (and subsequent neutralization or complexation) is a potential source of SOA. The reactants characterized in this work are precursors for aqueous chemistry and are potentially

400   important SOA_{AQ} precursors in all atmospheric waters, i.e. clouds, fogs, and wet aerosols.

The aqueous chemistry of these precursors is poorly understood and warrants further study.

4 Conclusions

405   We observed formation of pyruvate, oxalate, and acetate/glyocolate during OH oxidation experiments conducted with ambient mixtures of WSOG from the southeastern US. The formation of these highly oxygenated organic acids indicates a potential for SOA_{AQ} formation (e.g., upon neutralization with NH_3, metal complexation or heterogeneous reaction on course dust/salt particles). Given the acidity of SOAS fine

410   particles, we think it is unlikely that oxalate will be found in substantial quantities in the fine aerosol at the SOAS ground site.

We tentatively characterized several water-soluble reactive precursors which undergo aqueous chemistry and SOA_{AQ} formation in wet aerosols, clouds and fogs at this location. High resolution mass spectrometric analyses suggest precursors had O:C

415   ranging from 0.125-0.80 and some are tentatively gas-phase oxidation products of green leaf volatiles. No distinct difference was seen in the aqueous oxidation of ambient samples collected across days during the SOAS field campaign. Further work involving organic synthesis, aqueous OH oxidation of authentic standards, and mass spectral analyses with pre-separation are likely to yield further insights into the aqueous chemistry

420   of these compounds in the future.

5 Acknowledgements

This research was funded by the EPA STAR grant 835412. The views expressed in this

manuscript are those of the authors and do not necessarily reflect the views or policies of

425   the U.S. Environmental Protection Agency. The authors acknowledge Melissa Soule and

funding sources of the WHOI FT-MS User's Facility (NSF OCE-0619608 and the

Gordon and Betty Moore Foundation). We also thank Jeffrey Kirland, Ronald Lauck, and

Nancy Sazo for their invaluable assistance in the laboratory and field, and Louisa

Emmons for the air quality forecasting during SOAS.

430

Supporting Information Available. Included are sampling and TOC data for all collection

days (Table S1), time series of ESI-MS abundances for m/z+ 125, 129, 143, 173, and 187

(Figure S1), discussion and graphical comparisons with chemical ionization mass

spectrometry (CIMS) (Figure S2), and concentration dynamics for acetate+glycolate

435   during aqueous OH experiments and control experiments (Figure S3). The material is

available free of charge via the Internet at http://pubs.acs.org.

References

Altieri, K. E., Carlton, A. G., Lim, H.-J., Turpin, B. J., and Seitzinger, S. P.:

440   Evidence for Oligomer Formation in Clouds: Reactions of Isoprene Oxidation Products,

Environmental Science & Technology, 40, 4956-4960, 10.1021/es052170n, 2006.

Anderson, C., Dibb, J. E., Griffin, R. J., and Bergin, M. H.: Simultaneous

measurements of particulate and gas-phase water-soluble organic carbon concentrations

at remote and urban-influenced locations, Geophysical Research Letters, 35, L13706,

445   10.1029/2008GL033966, 2008a.

Anderson, C. H., Dibb, J. E., Griffin, R. J., Hagler, G. S. W., and Bergin, M. H.: Atmospheric water-soluble organic carbon measurements at Summit, Greenland, Atmospheric Environment, 42, 5612-5621, http://dx.doi.org/10.1016/j.atmosenv.2008.03.006, 2008b.

450 Blando, J. D., and Turpin, B. J.: Secondary organic aerosol formation in cloud and fog droplets: a literature evaluation of plausibility, Atmospheric Environment, 34, 1623-1632, 2000.

Boris, A. J., Desyaterik, Y., and Collett, J. L.: How do components of real cloud water affect aqueous pyruvate oxidation?, Atmos Res, 143, 95-106, DOI

455 10.1016/j.atmosres.2014.02.004, 2014.

Carlton, A. G., Turpin, B. J., Lim, H. J., Altieri, K. E., and Seitzinger, S.: Link between isoprene and secondary organic aerosol (SOA): Pyruvic acid oxidation yields low volatility organic acids in clouds, Geophysical Research Letters, 33, Artn L06822 Doi 10.1029/2005gl025374, 2006.

460 Carlton, A. G., Turpin, B. J., Altieri, K. E., Seitzinger, S. P., Mathur, R., Roselle, S. J., and Weber, R. J.: CMAQ Model Performance Enhanced When In-Cloud Secondary Organic Aerosol is Included: Comparisons of Organic Carbon Predictions with Measurements, Environmental Science & Technology, 42, 8798-8802, 2008.

Carlton, A. G., and Turpin, B. J.: Particle partitioning potential of organic

465 compounds is highest in the Eastern US and driven by anthropogenic water, Atmos. Chem. Phys., 13, 10203-10214, 10.5194/acp-13-10203-2013, 2013.

Crahan, K. K., Hegg, D., Covert, D. S., and Jonsson, H.: An exploration of aqueous oxalic acid production in the coastal marine atmosphere, Atmospheric

Environment, 38, 3757-3764, http://dx.doi.org/10.1016/j.atmosenv.2004.04.009,

470   2004.

De Haan, D. O., Corrigan, A. L., Smith, K. W., Stroik, D. R., Turley, J. J., Lee, F.

E., Tolbert, M. A., Jimenez, J. L., Cordova, K. E., and Ferrell, G. R.: Secondary Organic

Aerosol-Forming Reactions of Glyoxal with Amino Acids, Environmental Science &

Technology, 43, 2818-2824, 2009a.

475   De Haan, D. O., Tolbert, M. A., and Jimenez, J. L.: Atmospheric condensed-

phase reactions of glyoxal with methylamine, Geophysical Research Letters, 36,

doi:10.1029/2009GL037441, 2009b.

Dibb, J. E., Talbot, R. W., and Bergin, M. H.: Soluble acidic species in air and

snow at Summit, Greenland, Geophysical Research Letters, 21, 1627-1630,

480   10.1029/94GL01031, 1994.

Donahue, N. M., Robinson, A. L., Stanier, C. O., and Pandis, S. N.: Coupled

Partitioning, Dilution, and Chemical Aging of Semivolatile Organics, Environmental

Science & Technology, 40, 2635-2643, 10.1021/es052297c, 2006.

El Haddad, I., Yao, L., Nieto-Gligorovski, L., Michaud, V., Temime-Roussel, B.,

485   Quivet, E., Marchand, N., Sellegri, K., and Monod, A.: In-cloud processes of

methacrolein under simulated conditions - Part 2: Formation of secondary organic

aerosol, Atmos. Chem. Phys., 9, 5107-5117, 10.5194/acp-9-5107-2009, 2009.

Ervens, B., Feingold, G., Frost, G. J., and Kreidenweis, S. M.: A modeling study

of aqueous production of dicarboxylic acids: 1. Chemical pathways and speciated organic

490   mass production, Journal of Geophysical Research: Atmospheres, 109, n/a-n/a,

10.1029/2003JD004387, 2004.

Ervens, B., Carlton, A. G., Turpin, B. J., Altieri, K. E., Kreidenweis, S. M., and Feingold, G.: Secondary organic aerosol yields from cloud-processing of isoprene oxidation products, Geophysical Research Letters, 35, n/a-n/a, 10.1029/2007GL031828, 2008.

495

Ervens, B., Turpin, B. J., and Weber, R. J.: Secondary organic aerosol formation in cloud droplets and aqueous particles (aqSOA): a review of laboratory, field and model studies, Atmos. Chem. Phys., 11, 11069-11102, 10.5194/acp-11-11069-2011, 2011.

Ervens, B., Wang, Y., Eagar, J., Leaitch, W. R., Macdonald, A. M., Valsaraj, K.

500

T., and Herckes, P.: Dissolved organic carbon (DOC) and select aldehydes in cloud and fog water: the role of the aqueous phase in impacting trace gas budgets, Atmos. Chem. Phys., 13, 5117-5135, 10.5194/acp-13-5117-2013, 2013.

Foley, K. M., Roselle, S. J., Appel, K. W., Bhave, P. V., Pleim, J. E., Otte, T. L., Mathur, R., Sarwar, G., Young, J. O., Gilliam, R. C., Nolte, C. G., Kelly, J. T., Gilliland,

505

A. B., and Bash, J. O.: Incremental testing of the Community Multiscale Air Quality (CMAQ) modeling system version 4.7, Geosci. Model Dev., 3, 205-226, 10.5194/gmd-3-205-2010, 2010.

Fu, T.-M., Jacob, D. J., Wittrock, F., Burrows, J. P., Vrekoussis, M., and Henze, D. K.: Global budgets of atmospheric glyoxal and methylglyoxal, and implications for

510

formation of secondary organic aerosols, Journal of Geophysical Research: Atmospheres, 113, n/a-n/a, 10.1029/2007JD009505, 2008.

Fu, T.-M., Jacob, D. J., and Heald, C. L.: Aqueous-phase reactive uptake of dicarbonyls as a source of organic aerosol over eastern North America, Atmospheric

Environment, 43, 1814-1822, http://dx.doi.org/10.1016/j.atmosenv.2008.12.029,

515   2009.

Galloway, M. M., Chhabra, P. S., Chan, A. W. H., Surratt, J. D., Flagan, R. C.,

Seinfeld, J. H., and Keutsch, F. N.: Glyoxal uptake on ammonium sulphate seed aerosol:

reaction products and reversibility of uptake under dark and irradiated conditions, Atmos.

Chem. Phys., 9, 3331-3345, 10.5194/acp-9-3331-2009, 2009.

520   Gaston, C. J., Thornton, J. A., and Ng, N. L.: Reactive uptake of N2O5 to

internally mixed inorganic and organic particles: the role of organic carbon oxidation

state and inferred organic phase separations, Atmos. Chem. Phys., 14, 5693-5707,

10.5194/acp-14-5693-2014, 2014.

Goldstein, A. H., Koven, C. D., Heald, C. L., and Fung, I. Y.: Biogenic carbon

525   and anthropogenic pollutants combine to form a cooling haze over the southeastern

United States, Proceedings of the National Academy of Sciences, 106, 8835-8840,

10.1073/pnas.0904128106, 2009.

Gong, W., Stroud, C., and Zhang, L.: Cloud Processing of Gases and Aerosols in

Air Quality Modeling, Atmosphere, 2, 567-616, 2011.

530   Guo, H., Xu, L., Bougiatioti, A., Cerully, K. M., Capps, S. L., Hite Jr, J. R.,

Carlton, A. G., Lee, S. H., Bergin, M. H., Ng, N. L., Nenes, A., and Weber, R. J.: Fine-

particle water and pH in the southeastern United States, Atmos. Chem. Phys., 15, 5211-

5228, 10.5194/acp-15-5211-2015, 2015.

Hallquist, M., Wenger, J. C., Baltensperger, U., Rudich, Y., Simpson, D., Claeys,

535   M., Dommen, J., Donahue, N. M., George, C., Goldstein, A. H., Hamilton, J. F.,

Herrmann, H., Hoffmann, T., Iinuma, Y., Jang, M., Jenkin, M. E., Jimenez, J. L.,

Kiendler-Scharr, A., Maenhaut, W., McFiggans, G., Mentel, T. F., Monod, A., Prévôt, A. S. H., Seinfeld, J. H., Surratt, J. D., Szmigielski, R., and Wildt, J.: The formation, properties and impact of secondary organic aerosol: current and emerging issues, Atmos.

540   Chem. Phys., 9, 5155-5236, 10.5194/acp-9-5155-2009, 2009.

He, C., Liu, J., Carlton, A. G., Fan, S., Horowitz, L. W., Levy Ii, H., and Tao, S.: Evaluation of factors controlling global secondary organic aerosol production from cloud processes, Atmos. Chem. Phys., 13, 1913-1926, 10.5194/acp-13-1913-2013, 2013.

Heald, C. L., Jacob, D. J., Turquety, S., Hudman, R. C., Weber, R. J., Sullivan, A.

545   P., Peltier, R. E., Atlas, E. L., de Gouw, J. A., Warneke, C., Holloway, J. S., Neuman, J. A., Flocke, F. M., and Seinfeld, J. H.: Concentrations and sources of organic carbon aerosols in the free troposphere over North America, Journal of Geophysical Research: Atmospheres, 111, n/a-n/a, 10.1029/2006JD007705, 2006.

Hennigan, C. J., Bergin, M. H., Russell, A. G., Nenes, A., and Weber, R. J.:

550   Gas/particle partitioning of water-soluble organic aerosol in Atlanta, Atmos. Chem. Phys., 9, 3613-3628, 10.5194/acp-9-3613-2009, 2009.

Herrmann, H., Tilgner, A., Barzaghi, P., Majdik, Z., Gligorovski, S., Poulain, L., and Monod, A.: Towards a more detailed description of tropospheric aqueous phase organic chemistry: CAPRAM 3.0, Atmospheric Environment, 39, 4351-4363,

555   http://dx.doi.org/10.1016/j.atmosenv.2005.02.016, 2005.

Jiménez, E., Lanza, B., Antiñolo, M., and Albaladejo, J.: Influence of temperature on the chemical removal of 3-methylbutanal, trans-2-methyl-2-butenal, and 3-methyl-2-butenal by OH radicals in the troposphere, Atmospheric Environment, 43, 4043-4049, http://dx.doi.org/10.1016/j.atmosenv.2009.05.005, 2009.

560   Kalberer, M., Paulsen, D., Sax, M., Steinbacher, M., Dommen, J., Prevot, A. S. H., Fisseha, R., Weingartner, E., Frankevich, V., Zenobi, R., and Baltensperger, U.: Identification of Polymers as Major Components of Atmospheric Organic Aerosols, Science, 303, 1659-1662, 10.1126/science.1092185, 2004.

Kawamura, K., and Ikushima, K.: Seasonal changes in the distribution of

565   dicarboxylic acids in the urban atmosphere, Environmental Science & Technology, 27, 2227-2235, 10.1021/es00047a033, 1993.

Kawamura, K., Kasukabe, H., and Barrie, L. A.: Source and reaction pathways of dicarboxylic acids, ketoacids and dicarbonyls in arctic aerosols: One year of observations, Atmospheric Environment, 30, 1709-1722,

570   http://dx.doi.org/10.1016/1352-2310(95)00395-9, 1996.

Kawamura, K., Umemoto, N., Mochida, M., Bertram, T., Howell, S., and Huebert, B. J.: Water-soluble dicarboxylic acids in the tropospheric aerosols collected over east Asia and western North Pacific by ACE-Asia C-130 aircraft, Journal of Geophysical Research: Atmospheres, 108, 8639, 10.1029/2002JD003256, 2003.

575   Krechmer, J. E., Pagonis, D., Ziemann, P. J., and Jimenez, J. L.: Quantification of Gas-Wall Partitioning in Teflon Environmental Chambers Using Rapid Bursts of Low-Volatility Oxidized Species Generated in Situ, Environmental Science & Technology, 50, 5757-5765, 10.1021/acs.est.6b00606, 2016.

Kroll, J. H., Ng, N. L., Murphy, S. M., Varutbangkul, V., Flagan, R. C., and

580   Seinfeld, J. H.: Chamber studies of secondary organic aerosol growth by reactive uptake of simple carbonyl compounds, J.Geophys.Res., 110, D23207, 2005.

Lanza, B., Jiménez, E., Ballesteros, B., and Albaladejo, J.: Absorption cross section determination of biogenic C5-aldehydes in the actinic region, Chemical Physics Letters, 454, 184-189, http://dx.doi.org/10.1016/j.cplett.2008.02.020, 2008.

585   Lee, A. K. Y., Zhao, R., Gao, S. S., and Abbatt, J. P. D.: Aqueous-Phase OH Oxidation of Glyoxal: Application of a Novel Analytical Approach Employing Aerosol Mass Spectrometry and Complementary Off-Line Techniques, The Journal of Physical Chemistry A, 115, 10517-10526, 10.1021/jp204099g, 2011.

Lee, A. K. Y., Hayden, K. L., Herckes, P., Leaitch, W. R., Liggio, J., Macdonald, 590   A. M., and Abbatt, J. P. D.: Characterization of aerosol and cloud water at a mountain site during WACS 2010: secondary organic aerosol formation through oxidative cloud processing, Atmos. Chem. Phys., 12, 7103-7116, 10.5194/acp-12-7103-2012, 2012.

Liggio, J., Li, S. M., and McLaren, R.: Heterogeneous reactions of glyoxal on particulate matter: Identification of acetals and sulfate esters, Environmental Science & 595   Technology, 39, 1532-1541, 2005.

Lim, H.-J., Carlton, A. G., and Turpin, B. J.: Isoprene Forms Secondary Organic Aerosol through Cloud Processing: Model Simulations, Environmental Science & Technology, 39, 4441-4446, 10.1021/es048039h, 2005.

Lim, Y. B., Tan, Y., Perri, M. J., Seitzinger, S. P., and Turpin, B. J.: Aqueous 600   chemistry and its role in secondary organic aerosol (SOA) formation, Atmos. Chem. Phys., 10, 10521-10539, 10.5194/acp-10-10521-2010, 2010.

Limbeck, A., Puxbaum, H., Otter, L., and Scholes, M. C.: Semivolatile behavior of dicarboxylic acids and other polar organic species at a rural background site (Nylsvley,

RSA), Atmospheric Environment, 35, 1853-1862, http://dx.doi.org/10.1016/S1352-

605   2310(00)00497-0, 2001.

Lin, G., Sillman, S., Penner, J. E., and Ito, A.: Global modeling of SOA: the use

of different mechanisms for aqueous-phase formation, Atmos. Chem. Phys., 14, 5451-

5475, 10.5194/acp-14-5451-2014, 2014.

Lin, P., Huang, X.-F., He, L.-Y., and Zhen Yu, J.: Abundance and size

610   distribution of HULIS in ambient aerosols at a rural site in South China, Journal of

Aerosol Science, 41, 74-87, http://dx.doi.org/10.1016/j.jaerosci.2009.09.001, 2010.

Liu, J., Horowitz, L. W., Fan, S., Carlton, A. G., and Levy, H.: Global in-cloud

production of secondary organic aerosols: Implementation of a detailed chemical

mechanism in the GFDL atmospheric model AM3, Journal of Geophysical Research:

615   Atmospheres, 117, n/a-n/a, 10.1029/2012JD017838, 2012.

Loeffler, K. W., Koehler, C. A., Paul, N. M., and De Haan, D. O.: Oligomer

formation in evaporating aqueous glyoxal and methyl glyoxal solutions, Environmental

Science & Technology, 40, 6318-6323, 2006.

Mader, B. T., and Pankow, J. F.: Gas/Solid Partitioning of Semivolatile Organic

620   Compounds (SOCs) to Air Filters. 3. An Analysis of Gas Adsorption Artifacts in

Measurements of Atmospheric SOCs and Organic Carbon (OC) When Using Teflon

Membrane Filters and Quartz Fiber Filters, Environmental Science & Technology, 35,

3422-3432, 10.1021/es0015951, 2001.

Martinelango, P. K., Dasgupta, P. K., and Al-Horr, R. S.: Atmospheric production

625   of oxalic acid/oxalate and nitric acid/nitrate in the Tampa Bay airshed: Parallel pathways,

Atmospheric Environment, 41, 4258-4269, http://dx.doi.org/10.1016/j.atmosenv.2006.05.085, 2007.

Monge, M. E., Rosenørn, T., Favez, O., Müller, M., Adler, G., Abo Riziq, A., Rudich, Y., Herrmann, H., George, C., and D'Anna, B.: Alternative pathway for

630   atmospheric particles growth, Proceedings of the National Academy of Sciences, 109, 6840-6844, 10.1073/pnas.1120593109, 2012.

Myriokefalitakis, S., Tsigaridis, K., Mihalopoulos, N., Sciare, J., Nenes, A., Kawamura, K., Segers, A., and Kanakidou, M.: In-cloud oxalate formation in the global troposphere: a 3-D modeling study, Atmos. Chem. Phys., 11, 5761-5782, 10.5194/acp-

635   11-5761-2011, 2011.

Nguyen, T. B., Lee, P. B., Updyke, K. M., Bones, D. L., Laskin, J., Laskin, A., and Nizkorodov, S. A.: Formation of nitrogen- and sulfur-containing light-absorbing compounds accelerated by evaporation of water from secondary organic aerosols, Journal of Geophysical Research: Atmospheres, 117, D01207, 10.1029/2011JD016944, 2012.

640   Nguyen, T. B., Crounse, J. D., Teng, A. P., St. Clair, J. M., Paulot, F., Wolfe, G. M., and Wennberg, P. O.: Rapid deposition of oxidized biogenic compounds to a temperate forest, Proceedings of the National Academy of Sciences, 112, E392-E401, 10.1073/pnas.1418702112, 2015.

Nguyen, T. K. V., Petters, M. D., Suda, S. R., Guo, H., Weber, R. J., and Carlton,

645   A. G.: Trends in particle-phase liquid water during the Southern Oxidant and Aerosol Study, Atmos. Chem. Phys., 14, 10911-10930, 10.5194/acp-14-10911-2014, 2014.

Noziere, B., Dziedzic, P., and Córdova, A.: Products and kinetics of the liquid-phase reaction of glyoxal catalyzed by ammonium ions (NH4+), The Journal of Physical Chemistry A, 113, 231-237, 2008.

650   Nozière, B., and Cordova, A.: A kinetic and mechanistic study of the amino acid catalyzed aldol condensation of acetaldehyde in aqueous and salt solutions, Journal of Physical Chemistry A, 112, 2827-2837, 2008.

Nozière, B., Ekström, S., Alsberg, T., and Holmström, S.: Radical-initiated formation of organosulfates and surfactants in atmospheric aerosols, Geophysical

655   Research Letters, 37, n/a-n/a, 10.1029/2009GL041683, 2010.

O'Connor, M. P., Wenger, J. C., Mellouki, A., Wirtz, K., and Munoz, A.: The atmospheric photolysis of E-2-hexenal, Z-3-hexenal and E,E-2,4-hexadienal, Physical Chemistry Chemical Physics, 8, 5236-5246, 10.1039/B611344C, 2006.

Odum, J. R., Hoffmann, T., Bowman, F., Collins, D., Flagan, R. C., and Seinfeld,

660   J. H.: Gas/Particle Partitioning and Secondary Organic Aerosol Yields, Environmental Science & Technology, 30, 2580-2585, 10.1021/es950943+, 1996.

Ortiz-Montalvo, D. L., Häkkinen, S. A. K., Schwier, A. N., Lim, Y. B., McNeill, V. F., and Turpin, B. J.: Ammonium Addition (and Aerosol pH) Has a Dramatic Impact on the Volatility and Yield of Glyoxal Secondary Organic Aerosol, Environmental

665   Science & Technology, 48, 255-262, 10.1021/es4035667, 2014.

Paciga, A. L., Riipinen, I., and Pandis, S. N.: Effect of Ammonia on the Volatility of Organic Diacids, Environmental Science & Technology, 48, 13769-13775, 10.1021/es5037805, 2014.

Paulot, F., Crounse, J. D., Kjaergaard, H. G., Kurten, A., St Clair, J. M., Seinfeld, J. H., and Wennberg, P. O.: Unexpected Epoxide Formation in the Gas-Phase Photooxidation of Isoprene, Science, 325, 730-733, DOI 10.1126/science.1172910, 2009.

Perri, M. J., Seitzinger, S., and Turpin, B. J.: Secondary organic aerosol production from aqueous photooxidation of glycolaldehyde: Laboratory experiments, Atmospheric Environment, 43, 1487-1497, http://dx.doi.org/10.1016/j.atmosenv.2008.11.037, 2009.

Perri, M. J., Lim, Y. B., Seitzinger, S. P., and Turpin, B. J.: Organosulfates from glycolaldehyde in aqueous aerosols and clouds: Laboratory studies, Atmospheric Environment, 44, 2658-2664, http://dx.doi.org/10.1016/j.atmosenv.2010.03.031, 2010.

Portmann, R. W., Solomon, S., and Hegerl, G. C.: Spatial and seasonal patterns in climate change, temperatures, and precipitation across the United States, Proceedings of the National Academy of Sciences, 106, 7324-7329, 10.1073/pnas.0808533106, 2009.

Robinson, W. A., Reudy, R., and Hansen, J. E.: General circulation model simulations of recent cooling in the east-central United States, Journal of Geophysical Research: Atmospheres, 107, ACL 4-1-ACL 4-14, 10.1029/2001JD001577, 2002.

Rossignol, S., Aregahegn, K. Z., Tinel, L., Fine, L., Nozière, B., and George, C.: Glyoxal Induced Atmospheric Photosensitized Chemistry Leading to Organic Aerosol Growth, Environ Sci Technol, 48, 3218-3227, 10.1021/es405581g, 2014.

Sareen, N., Schwier, A. N., Shapiro, E. L., Mitroo, D., and McNeill, V. F.: Secondary organic material formed by methylglyoxal in aqueous aerosol mimics, Atmos. Chem. Phys., 10, 997-1016, 10.5194/acp-10-997-2010, 2010.

Saxena, P., and Hildemann, L.: Water-soluble organics in atmospheric particles: A critical review of the literature and application of thermodynamics to identify candidate compounds, J Atmos Chem, 24, 57-109, 10.1007/BF00053823, 1996.

695   Schwier, A. N., Sareen, N., Mitroo, D., Shapiro, E. L., and McNeill, V. F.: Glyoxal-Methylglyoxal Cross-Reactions in Secondary Organic Aerosol Formation, Environmental Science & Technology, 44, 6174-6182, 10.1021/es101225q, 2010.

Seinfeld, J. H., and Pankow, J. F.: Organic atmospheric particulate material, Annu Rev Phys Chem, 54, 121-140, Doi 10.1146/Annurev.Physchem.54.011002.103756, 2003.

700   Shapiro, E. L., Szprengiel, J., Sareen, N., Jen, C. N., Giordano, M. R., and McNeill, V. F.: Light-absorbing secondary organic material formed by glyoxal in aqueous aerosol mimics, Atmospheric Chemistry and Physics, 9, 2289-2300, 2009.

Sorooshian, A., Varutbangkul, V., Brechtel, F. J., Ervens, B., Feingold, G., Bahreini, R., Murphy, S. M., Holloway, J. S., Atlas, E. L., Buzorius, G., Jonsson, H.,
705 Flagan, R. C., and Seinfeld, J. H.: Oxalic acid in clear and cloudy atmospheres: Analysis of data from International Consortium for Atmospheric Research on Transport and Transformation 2004, Journal of Geophysical Research: Atmospheres, 111, n/a-n/a, 10.1029/2005JD006880, 2006.

Sorooshian, A., Murphy, S. M., Hersey, S., Bahreini, R., Jonsson, H., Flagan, R.
710 C., and Seinfeld, J. H.: Constraining the contribution of organic acids and AMS m/z 44 to the organic aerosol budget: On the importance of meteorology, aerosol hygroscopicity, and region, Geophysical Research Letters, 37, n/a-n/a, 10.1029/2010GL044951, 2010.

Spaulding, R. S., Schade, G. W., Goldstein, A. H., and Charles, M. J.: Characterization of secondary atmospheric photooxidation products: Evidence for

715   biogenic and anthropogenic sources, Journal of Geophysical Research: Atmospheres,

108, n/a-n/a, 10.1029/2002JD002478, 2003.

Sun, Y. L., Zhang, Q., Anastasio, C., and Sun, J.: Insights into secondary organic

aerosol formed via aqueous-phase reactions of phenolic compounds based on high

resolution mass spectrometry, Atmos. Chem. Phys., 10, 4809-4822, 10.5194/acp-10-

720   4809-2010, 2010.

Surratt, J. D., Lewandowski, M., Offenberg, J. H., Jaoui, M., Kleindienst, T. E.,

Edney, E. O., and Seinfeld, J. H.: Effect of Acidity on Secondary Organic Aerosol

Formation from Isoprene, Environmental Science & Technology, 41, 5363-5369,

10.1021/es0704176, 2007.

725   Tan, Y., Perri, M. J., Seitzinger, S. P., and Turpin, B. J.: Effects of Precursor

Concentration and Acidic Sulfate in Aqueous Glyoxal−OH Radical Oxidation and

Implications for Secondary Organic Aerosol, Environmental Science & Technology, 43,

8105-8112, 10.1021/es901742f, 2009.

Tan, Y., Lim, Y. B., Altieri, K. E., Seitzinger, S. P., and Turpin, B. J.:

730   Mechanisms leading to oligomers and SOA through aqueous photooxidation: insights

from OH radical oxidation of acetic acid and methylglyoxal, Atmos. Chem. Phys., 12,

801-813, 10.5194/acp-12-801-2012, 2012.

Volkamer, R., Jimenez, J. L., San Martini, F., Dzepina, K., Zhang, Q., Salcedo,

D., Molina, L. T., Worsnop, D. R., and Molina, M. J.: Secondary organic aerosol

735   formation from anthropogenic air pollution: Rapid and higher than expected, Geophys.

Res. Lett., 33, L17811, 10.1029/2006gl026899, 2006.

Volkamer, R., Martini, F. S., Molina, L. T., Salcedo, D., Jimenez, J. L., and Molina, M. J.: A missing sink for gas-phase glyoxal in Mexico City: Formation of secondary organic aerosol, Geophysical Research Letters, 34, 10.1029/2007gl030752, 2007.

Volkamer, R., Ziemann, P. J., and Molina, M. J.: Secondary Organic Aerosol Formation from Acetylene (C_2H_2): seed effect on SOA yields due to organic photochemistry in the aerosol aqueous phase, Atmos. Chem. Phys., 9, 1907-1928, 10.5194/acp-9-1907-2009, 2009.

Yao, X., Fang, M., and Chan, C. K.: Size distributions and formation of dicarboxylic acids in atmospheric particles, Atmospheric Environment, 36, 2099-2107, http://dx.doi.org/10.1016/S1352-2310(02)00230-3, 2002.

Zhang, Z., Lin, Y. H., Zhang, H., Surratt, J. D., Ball, L. M., and Gold, A.: Technical Note: Synthesis of isoprene atmospheric oxidation products: isomeric epoxydiols and the rearrangement products cis- and trans-3-methyl-3,4-dihydroxytetrahydrofuran, Atmos. Chem. Phys., 12, 8529-8535, 10.5194/acp-12-8529-2012, 2012.

Tables & Figures

Table 1: Sample collection dates for which experiments were run and their sampling
conditions. Temperature, relative humidity, and ozone ranges are shown both for the
760 entire day and collection time period. Total organic carbon (TOC) accuracy and precision
are verified with potassium hydrogen phthalate (KHP) standards to be better than 5%
(Perri et al., 2009).

Collection date	Collection time	μM TOC	T (^{o}C) all day (coll. time)	RH (%) all day (coll. time)	O$_3$ (ppb$_V$) all day (coll. time)
11-Jun-2013	7am-7pm	139.5	22-32 (23-32)	53-99 (53-98)	9.9-38.2 (11.3-38.2)
12-Jun-2013	7am-7pm	179.7	23-33 (23-33)	48-94 (48-94)	13.1-41.8 (13.1-41.8)
15-Jun-2013	7am-7pm	117.0	17-31 (18-31)	45-94 (45-90)	11.6-53.4 (11.6-53.4)
16-Jun-2013	7am-7pm	108.2	22-32 (22-32)	53-93 (53-84)	2.6-41.7 (23.1-41.7)
20-Jun-2013	8am-5pm	131.5	20-30 (21-30)	55-98 (59-94)	4.8-52.2 (6.2-42.8)
21-Jun-2013	10am-6pm	104.4	20-30 (25-30)	50-93 (50-78)	16.6-45.2 (30.3-45.2)
29-Jun-2013	7am-7pm	92.0	21-31 (22-31)	43-100 (43-100)	16.3-53.7 (16.3-53.7)
30-Jun-2013	7am-7pm	98.7	20-30 (20-30)	38-100 (38-100)	1-53.5 (1-53.5)

765

Table 2: Elemental formulas assigned to precursor ions using ESI-FT-ICR MS in the positive ionization mode and Midas Molecular Formula Calculator. MS/MS fragmentation data is also shown.

Precursor peak using ESI-MS	Positive mode m/z (using FT-ICR)	[M+Na]+ or [M+H]+	Mol. Wt.	Double bond equivalents
187	187.0942	$C_7H_{16}O_4Na$	164.1043	0
	155.0680	$C_6H_{12}O_3Na$	132.0786	1
173	173.0782	$C_6H_{14}O_4Na$	150.0887	0
	141.0523	$C_5H_{10}O_3Na$	118.0625	1
	129.0524	$C_4H_{10}O_3Na$	106.0625	0
143	143.0676	$C_5H_{12}O_3Na$	120.0781	0
129	129.0520	$C_4H_{10}O_3Na$	106.0625	0
125	125.096	$C_8H_{13}O$	124.0883	3

770
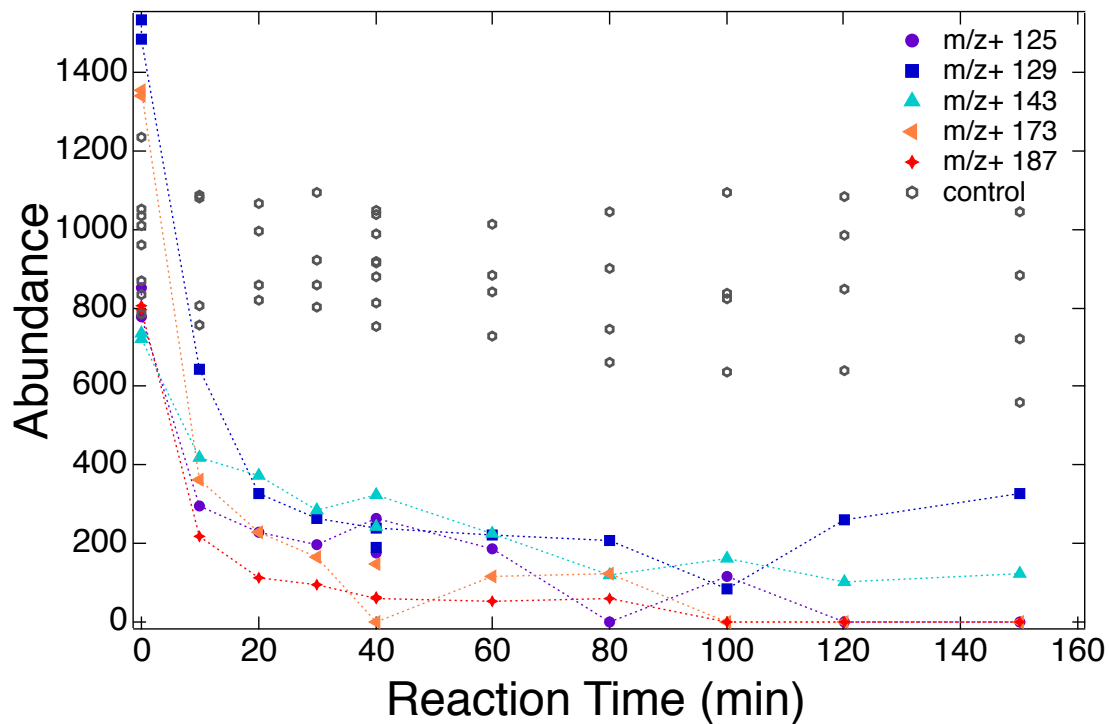
Figure 1. Positive ions (ESI-MS) exhibiting precursor-like trends during aqueous OH-radical oxidation experiments with the ambient mixtures collected on June 30. All days show similar trends, with all 5 reactant masses showing statistically significant decreasing trends as compared to the control experiments. Controls (sample + UV, sample + H_2O_2) shown for m/z 187; other masses show similar trends.

775

m/z+ 187

$C_7H_{16}O_4$

- CH₃OH
- 32

$C_6H_{12}O_3$

$C_6H_{12}O_3$ gas-phase

$C_6H_{14}O_4$ aqueous-phase
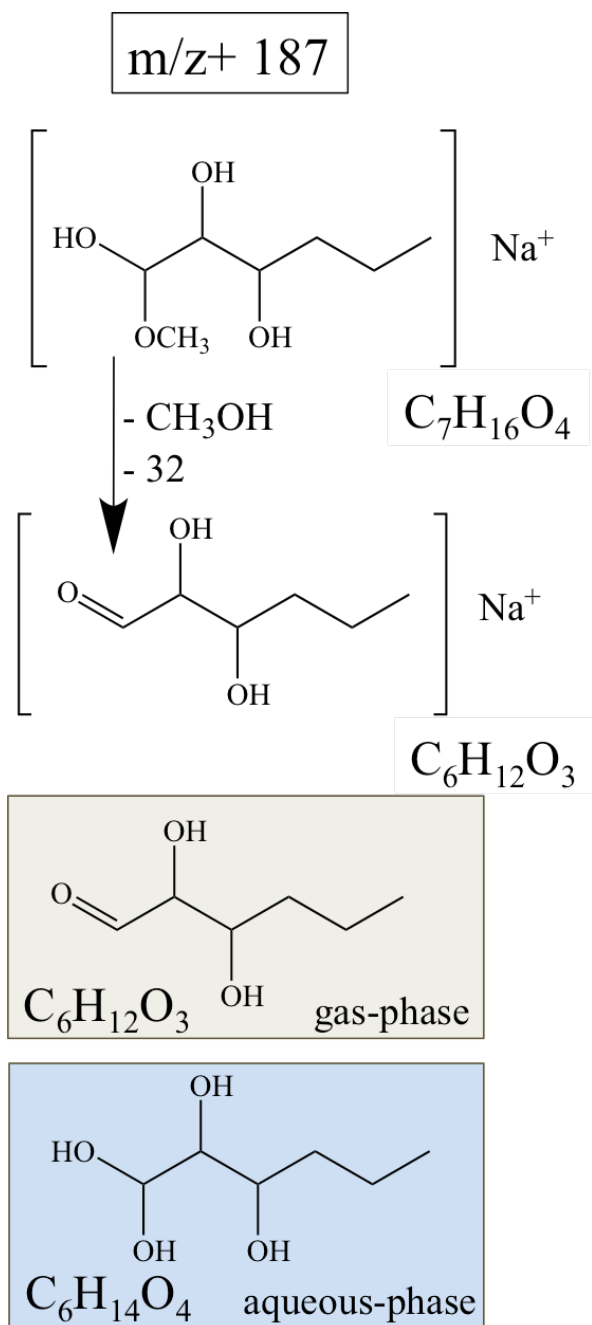
780

Figure 2. Proposed structure for the positive ion at *m/z* 187. The top structure is the parent compound detected as a reactant in the ESI-MS; the following structures show the MS/MS fragments. This compound would take the forms shown in the shaded boxes when present in atmospheric air and water.

m/z+ 173

$C_6H_{14}O_4$

- CH$_3$OH
- 32

$C_5H_{10}O_3$

- C$_2$H$_4$O
- 44

$C_4H_{10}O_3$

$C_5H_{10}O_3$ gas-phase

$C_5H_{12}O_4$ aqueous-phase
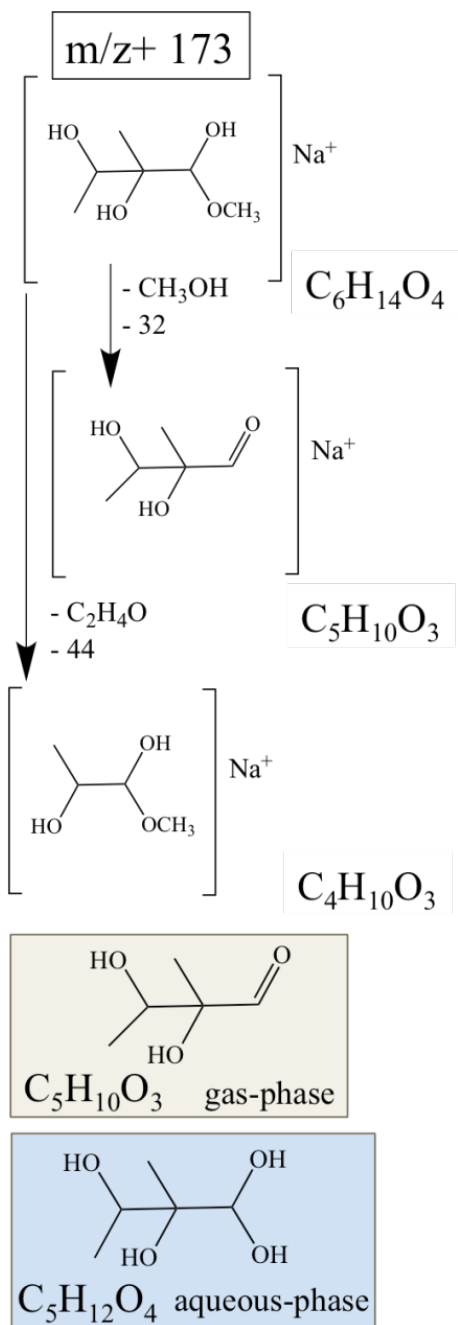
785

Figure 3. Proposed structure for the positive ion at *m/z* 173. The top structures in each panel are the parent compound detected as a reactant in the ESI-MS; the following structures show the MS/MS fragments. This compound would take the forms shown in the shaded boxes when present in atmospheric air and water.

790

(a)
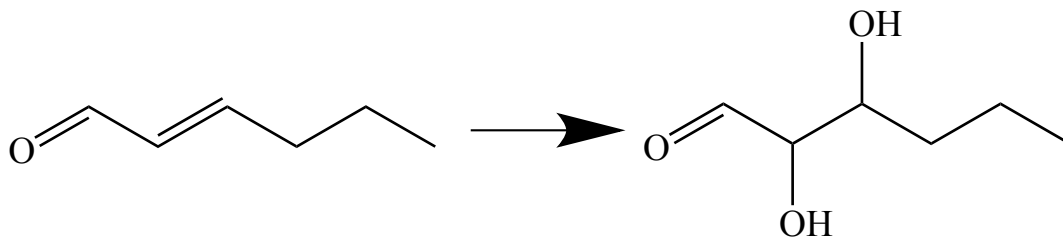
(b)
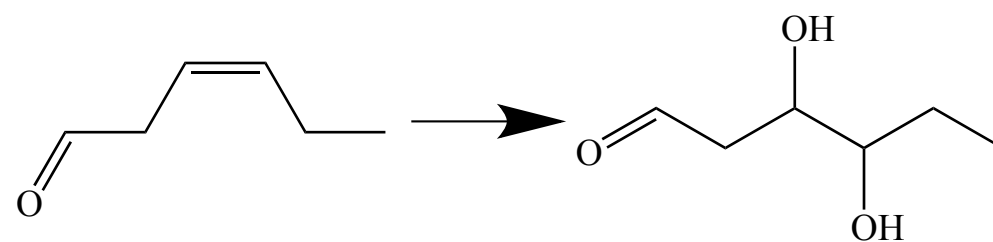
795

(c)
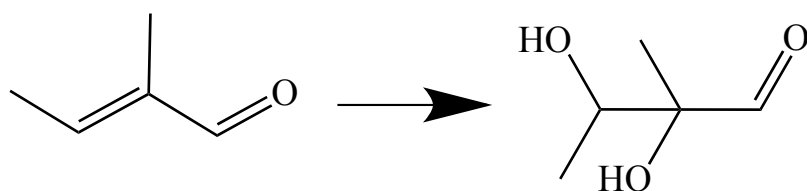
Figure 4: Gas-phase oxidation of (a) *E*-2-hexenal and (b) *Z*-3-hexenal and (c) (*E*)-2-methyl-2-butenal.

800
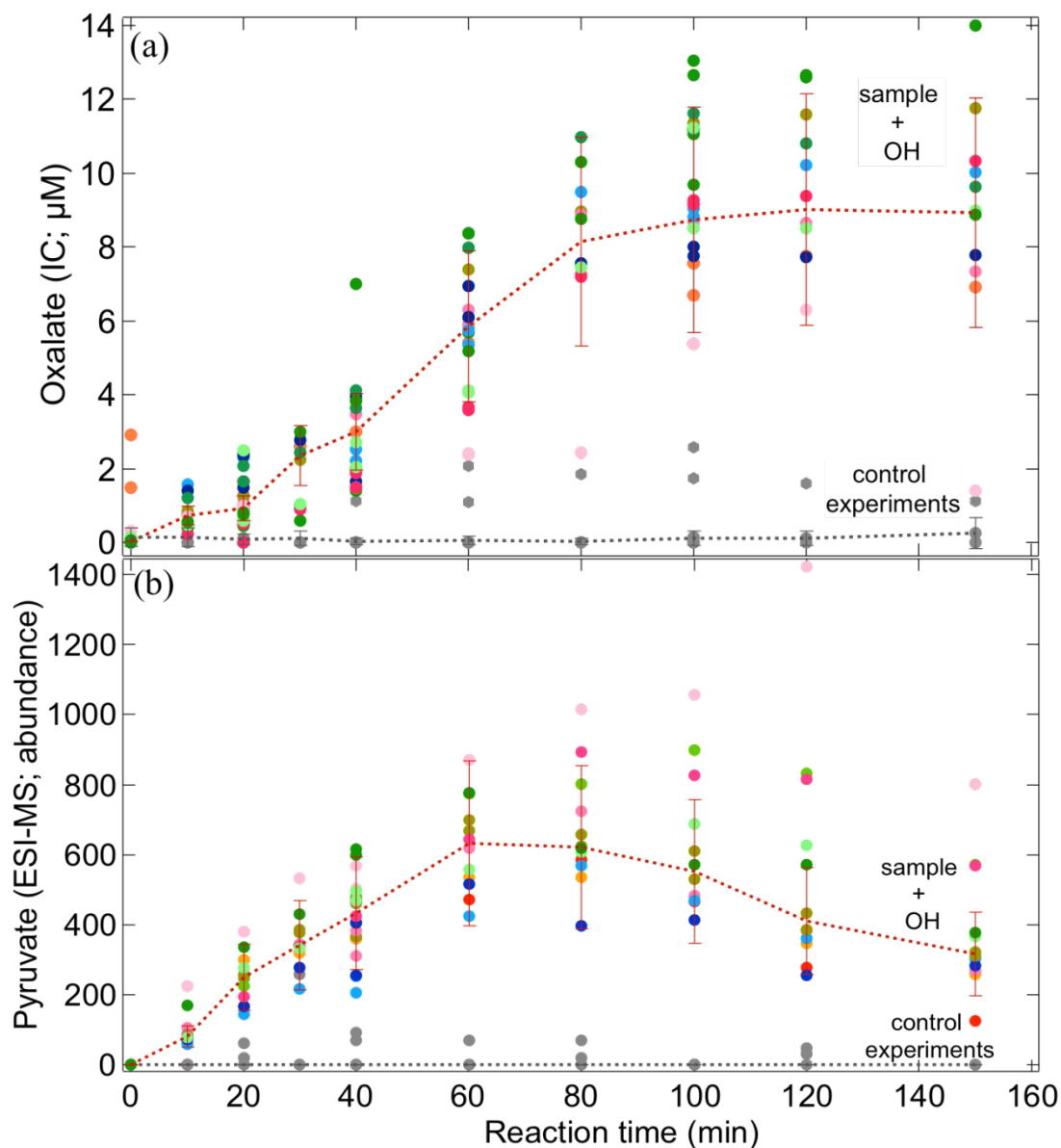
Figure 5. (a) Oxalate (by IC) for all OH radical oxidation experiments conducted with ambient samples (Table 1). (b) Abundance of the negative ion at *m/z* 87 (pyruvate) as observed in the ESI-MS when the ambient SOAS samples are exposed to OH. Error bars represent the pooled coefficient of variation calculated across experimental days. Note that oxalate and pyruvate are formed in all samples in the presence, but not the absence, of OH. Gray points represent control experiments (June 11 sample + UV, June 11 sample + H_2O_2, June 30 field water blank + OH).